EPJ manuscript No.
(will be inserted by the editor)

Studying Low-x Dynamics using the Hadronic Final State in DIS at HERA

Roman Pöschl [a] [b]

DESY, Notkestr. 85, D-22603 Hamburg

Received: February 7, 2008 / Revised version: February 7, 2008

Abstract. This article describes different approaches to investigate the behavior of parton evolution in the proton by exploiting various aspects of the hadronic final state produced in Deep Inelastic Scattering Events at HERA.

PACS. 13.60.Hb – 12.38.Qk

1 Introduction

Measurements of the hadronic final state in deeply inelastic ep scattering (DIS) provide precision tests of quantum chromodynamics (QCD). At HERA data are collected over a wide range of the negative four-momentum-transfer Q^2, the Bjorken variable x and the transverse momenta p_T of hadronic final state objects. Studies of the hadronic final state may be used to get insight into the dynamics of the parton cascade exchanged in low-x lepton proton interactions. Fig. 1 shows a generic DIS process in which a gluon from the proton undergoes a QCD cascade. The gluon interacts with the virtual photon via a hard photon-gluon process which can be calculated within perturbative QCD using an exact matrix element. The cascade itself represents an approximation for an all order matrix element calculation and several prescriptions to describe the QCD dynamics within the cascade have been proposed. The most familiar one is given by the so called DGLAP evolution equations [1]. In these equations the large logarithms in Q^2 are resummed, neglecting $\log(1/x)$ terms. This practically corresponds to a strong ordering of the transverse momenta of the emitted partons, *i.e.* $k_{t,1} << .. << k_{t,n} << .. << Q^2$. DGLAP evolution is expected to break down at sufficiently low values of x, when the ordering no longer applies.

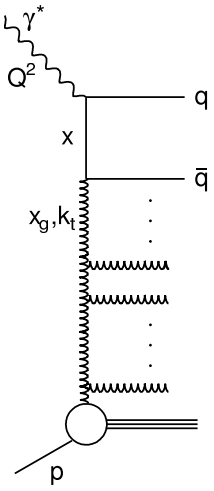

Fig. 1. Diagram of a generic DIS process at low x. Here k_t denotes the transverse momenta of the exchanged gluons, x_g is the fractional momentum of the parton taking part in the hard interaction and x is the Bjorken scaling variable

At very low values of x it is believed that the theoretically most appropriate description is given by the BFKL evolution equations [2]. These resum large logarithms of $1/x$ up to all orders and impose no restriction on the ordering of the transverse momenta within the parton cascade. Thus off-shell matrix elements have to be used together with an unintegrated gluon distribution function, $f(x, \tilde{\mu}_f^2, k_t)$, which depends on the gluon transverse momentum k_t as well as x and a hard scale $\tilde{\mu}_f$. A promising approach to parton evolution at both low and large values of x is given by the CCFM [3] evolution equation, which, by means of angular-ordered parton emission, is equivalent to the BFKL ansatz for $x \to 0$, while reproducing the DGLAP equations at large x.

2 Forward π^0/Jet Cross Sections

An extended parton ladder at low x leads to high k_t partonic emission in the region close to the proton remnant ('forward' region) to which measurements of jets and leading particles, *e.g.* π^0 are sensitive. Production of a forward π^0 can be regarded as a refined version of forward jet production. In order to enhance the sensitivity to low-x effects special selection cuts have been applied such as confining the ratio $p^2_{T,(\pi^0,Jet)}/Q^2$ to values between 0.5 and 2 inspired by a proposal in [4].

2.1 Forward π^0 Cross Sections

Inclusive forward π^0 cross sections for transverse momenta $p_{T,\pi^0} > 3.5$ GeV are shown in Fig. 2 as a function of x

[a] For the H1 and ZEUS Collaborations
[b] Talk presented at the EPS03, Aachen, July 2003

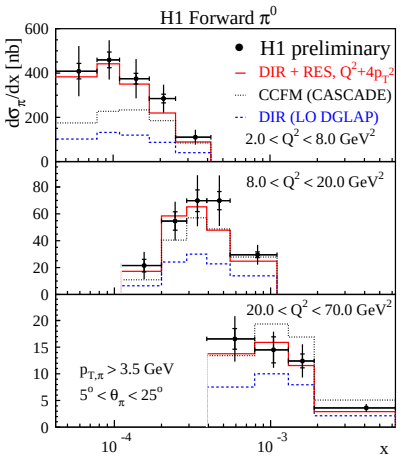

Fig. 2. Forward π^0 cross section as a function of Bjorken-x in different regions of Q^2 compared with predictions of DGLAP and CCFM based QCD Models.

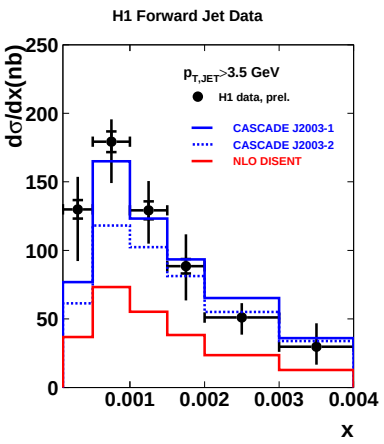

Fig. 3. Forward jet cross section as a function of Bjorken-x compared with NLO DGLAP QCD calculations and predictions by the CCFM Model CASCADE.

for different regions of Q^2. The data are compared with predictions of the Monte Carlo models RAPGAP [5] and CASCADE [6]. RAPGAP implements a QCD model based on Leading Order ($O(\alpha_s)$, LO) parton showers with ('DIR +RES') and without ('DIR') resolved photon structure. CASCADE is employed as an implementation of the CCFM evolution equation introduced above. The prediction by RAPGAP with a pointlike photon (DIR) is well below the data. A reasonable description of the data is achieved by including contributions from resolved virtual photons in the predictions and using a factorization scale of $Q^2 + 4p_{T,\pi^0}$. Note, that resolved contributions can be considered to mimic a lack of ordering in transverse momentum as required for a DGLAP evolution scheme. CASCADE predictions based on the unintegrated gluon density JS2001 [6] on the other hand undershoot the data for lower values of Q^2.

2.2 Forward Jet Cross Sections

Results complementary to the ones discussed in Sec. 2.1 are obtained by studying jets in the same region of phase space. Jets are reconstructed with the longitudinally invariant k_t cluster algorithm [7]. Fig. 3 shows the forward jet cross section for transverse momenta $p_{T,Jet} > 3.5$ GeV as a function of x. The data are compared with NLO ($O(\alpha_s^2)$) QCD calculations performed with the program DISENT [9] and predictions by CASCADE based on two recent sets of unintegrated gluon distributions [8]. While results of the NLO QCD calculations are significantly below the data, the CASCADE prediction based on the set labelled J2003-1 is in good agreement with the data. The difference between the CASCADE predictions indicates the sensitivity of forward jet data to low-x dynamics.

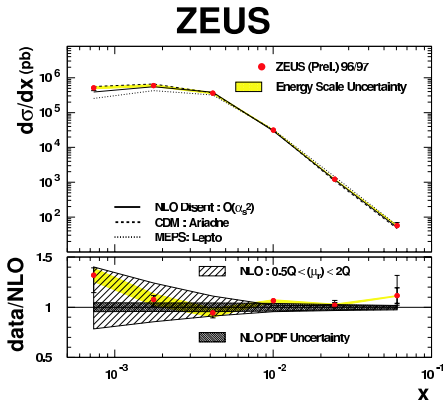

Fig. 4. Inclusive jet cross section as a function of Bjorken-x compared with NLO DGLAP QCD predictions and DGLAP based QCD Models.

3 Inclusive Jet Cross Sections

In the following analysis of inclusive jet cross sections the restriction to the forward region and the kinematic confinement introduced in Sec. 2 are removed, leading to a somewhat more general study of jet cross sections. In [10] it is outlined that the comparison of the measured jet cross sections with matrix element calculations including contributions up to $O(\alpha_s)$ performed with DISENT lead to significant discrepancies between the data and the theoretical predictions. If, however, hadronic activity in the forward and the backward hemisphere is required and NLO ($O(\alpha_s^2)$) predictions are employed a much better agreement between the data and the theoretical prediction is obtained, which is demonstrated in Fig. 4. The theoretical error represented by the hatched band is due to missing higher order contributions in the theoretical calculations. Predictions based on LO DGLAP parton showers, here represented by LEPTO [11], undershoot the data at low-x while a good description of the data is obtained by the CDM [12] model as implemented in the event generator ARIADNE [13].

4 Azimuthal Correlations between Jets

Insight into low-x dynamics can be gained from inclusive dijet data by studying the behavior of events with a small azimuthal separation, $\Delta\phi^*$, between the two hardest jets as measured in the hadronic center-of-mass system [14–16]. Partons entering the hard scattering process with negligible transverse momentum, k_t, as assumed in the DGLAP formalism, lead at leading order to a back-to-back configuration of the two outgoing jets with $\Delta\phi^* = 180°$. Azimuthal jet separations different from 180° occur due to higher order QCD effects. However, in models which predict a significant proportion of partons entering the hard process with large k_t, the number of events with small $\Delta\phi^*$ should also increase.

Here we present a measurement of the ratio

$$S = \frac{\int_0^{120^\circ} N_{\mathrm{dijet}}(\Delta\phi^*, x, Q^2)\mathrm{d}\Delta\phi^*}{\int_0^{180^\circ} N_{\mathrm{dijet}}(\Delta\phi^*, x, Q^2)\mathrm{d}\Delta\phi^*},$$

of the number of events N_{dijet} with an azimuthal jet separation of $\Delta\phi^* < 120°$ relative to all dijet events. The observable was proposed in [16] and is considered to be directly sensitive to low-x effects.

Fig. 5 presents the S-distribution as a function of x for different Q^2. It is of the order of 5% and increases with decreasing x. This rise of S is most prominent in the lowest Q^2 bin, where the smallest values of x are reached. The NLO dijet QCD calculations, resulting in an effective LO prediction for S, predict S-values of only ∼1% and show no rise towards low x. NLO 3-jet predictions by the program NLOJET [17] which lead to an effective NLO prediction for S give a good description of the data at large Q^2 and large x, but still fail to describe the increase towards low x, particularly in the lowest Q^2 range. According to the discussion given in [18], predictions based on CCFM evolution as implemented in CASCADE lead to an improved overall agreement with the data in particular at low x and Q^2.

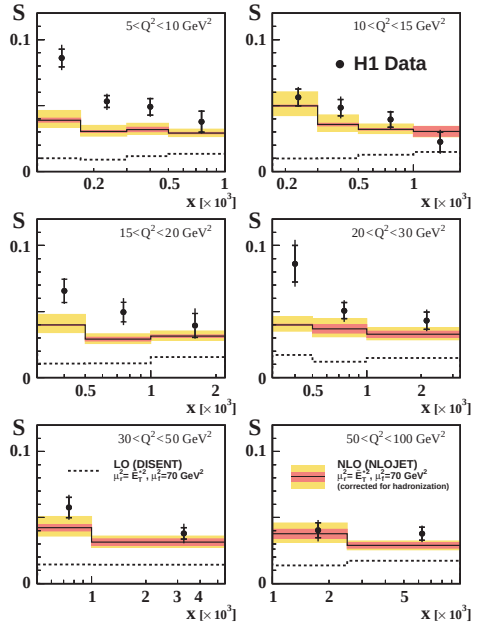

Fig. 5. The observable S given as a function of Bjorken-x and Q^2 compared with LO and NLO DGLAP QCD predictions.

References

1. V.N. Gribov and L.N. Lipatov, *Sov. J. Nucl. Phys.* **15** (1972) 438 and 675;
   L.N. Lipatov, *Sov. J. Nucl. Phys.* **20** (1975) 94;
   G. Altarelli and G. Parisi, *Nucl. Phys.* **B 126** (1977) 298;
   Y.L. Dokshitzer, *Sov. Phys. JETP* **46** (1977) 641.
2. V.S. Fadin, E.A. Kuraev and L.N. Lipatov, *Sov. Phys. JETP* **44** (1976) 443;
   V.S. Fadin, E.A. Kuraev and L.N. Lipatov, *Sov. Phys. JETP* **45** (1977) 199.
   Y. Balitsky and L.N. Lipatov, *Sov. J. Nucl. Phys.* **28** (1978) 822.
3. M. Ciafaloni, *Nucl. Phys.* **B 296** (1988) 49;
   S. Catani, F. Fiorani and G. Marchesini, *Phys. Lett.* **B 234** (1990) 339;
   S. Catani, F. Fiorani and G. Marchesini, *Nucl. Phys.* **B 336** (1990) 18;
   G. Marchesini, *Nucl. Phys.* **B 445** (1995) 49 [hep-ph/9412327].
4. A.H. Mueller, *Nucl.Phys.Proc.Suppl.*, **C 18** (125) 1991;
   J.Phys **G 17** (1443) 1991.
5. H. Jung, *Comp. Phys. Commun.* **86** (1995) 147;
   H. Jung, *The RAPGAP Monte Carlo for Deep Inelastic Scattering, version 2.08*, Lund University, 1999,
   `http://www.desy.de/~jung/rapgap.html`.
6. H. Jung and G.P. Salam, *Eur. Phys. J.* **C 19** (2001) 351 [hep-ph/0012143];
   H. Jung, *Comp. Phys. Commun.* **143** (2002) 100 [hep-ph/0109102].
7. S.D. Ellis and D.E. Soper, *Phys. Rev.* **D 48** (1993) 3160 [hep-ph/9305266];
   S. Catani *et al.*, *Nucl. Phys.* **B 406** (1993) 187.
8. M. Hansson and H. Jung, [hep-ph/0309009].
9. S. Catani and M.H. Seymour, *Nucl. Phys.* **B485** (1997) 291, *Erratum-ibid.* B **510** (1997) 503 [hep-ph/9605323].
   L. Lönnblad, *Comp. Phys. Commun.* **71** (1992) 15.
10. ZEUS Collaboration, Contributed paper No. 507 to the International Europhysics Conference on High Energy Physics, EPS03, July 2003 Aachen, Germany.
11. G. Ingelman, A. Edin and J. Rathsman, *Comp. Phys. Commun.* **101** (1997) 108 [hep-ph/9605286].
12. B. Andersson, G. Gustafson and L. Lönnblad, *Nucl. Phys.* **B 339** (1990) 393.
13. L. Lönnblad, *Comp. Phys. Commun.* **71** (1992) 15.
14. J.R. Forshaw and R.G. Roberts, *Phys. Lett.* **B 335** (1994) 494 [hep-ph/9403363] ;
    J. Kwieciński, A.D. Martin and A.M. Staśto, *Phys. Lett.* **B 459** (1999) 644 [hep-ph/9904402].
15. A.J. Askew *et al.*, *Phys. Lett.* **B 338** (1994) 92 [hep-ph/9407337].
16. A. Szczurek *et al.*, *Phys. Lett.* **B 500** (2001) 254 [hep-ph/0011281].
17. Z. Nagy and Z. Trocsanyi, *Phys. Rev. Lett.* **87** (2001) 082001 [hep-ph/0104315].
18. H1 Collaboration, paper submitted to *Eur. Phys. J.* **C** [hep-ex/0310019].